Influence of 4H-SiC substrate miscut on the epitaxy and microstructure of AlGaN/GaN heterostructures

Growth and microstructural characterization of AlGaN/GaN heterostructures grown on low angle-off 4H-SiC substrates

A.Gkanatsiou[1)], Ch. B. Lioutas[1)], N. Frangis[1)], E. K. Polychroniadis[1)],

, P. Prystawko[3, 4)], M.Leszczynski[4, 3)], Th. Altantzis[2)], G. Van Tendeloo[2)]

[1)] Department of Physics, Aristotle University of Thessaloniki 54124, Greece
[2)] Electron Microscopy for Materials Science (EMAT), University of Antwerp, Groenenborgerlaan 171, 2020 Antwerp, Belgium
[3)] Institute of High Pressure Physics "Unipress", Polish Academy of Sciences Sokolowska 29/37, 01-142 Warsaw, Poland
[4)]TopGaN Ltd Sokolowska 29/37, 01-142 Warsaw, Poland

Abstract.
AlGaN/GaN heterostructures were grown on "on-axis" and 2° off (0001) 4H-SiC substrates by metalorganic vapor phase epitaxy (MOVPE). Structural characterization was performed by transmission electron microscopy. The dislocation density, being greater in the on-axis case, is gradually reduced in the GaN layer and is forming dislocation loops in the lower region. Steps aligned along $[1\bar{1}00]$ in the off-axis case give rise to simultaneous defect formation. In the on-axis case, an almost zero density of steps is observed, with the main origin of defects probably being the orientation mismatch at the grain boundaries between the small not fully coalesced AlN grains. V-shaped formations are observed in the AlN nucleation layer, but are more frequent in the off-axis case, probably enhanced by the presence of steps. These V-shaped formations are completely overgrown by the GaN layer, during the subsequent deposition, presenting AlGaN areas in the walls of the defect, indicating an inter-diffusion between the layers. Finally, at the AlGaN/GaN heterostructure surface in the on-axis case, V-shapes are observed, with the AlGaN (21% Al) thickness exceeding the critical for relaxation thickness. On the other hand, no relaxation in the form of V-shape creation is observed in the off-axis case, probably due to the smaller AlGaN thickness (less than 21% Al). The AlN spacer layer, grown in between the heterostructure, presents a uniform thickness and clear interfaces.

Keywords: AlGaN/GaN; heterostructure; TEM; HRTEM; STEM; High Electron Mobility Transistor; SiC substrate.

1. Introduction

Wide band gap semiconductors (silicon carbide (SiC) and gallium nitride (GaN)), offer great advantages, making them ideal candidates for high power and frequency applications: they combine a wide band gap, a high breakdown field (over 3.75MV/cm for GaN), a high saturation velocity and they possess the ability to form high quality AlGaN/GaN heterostructures with good transport properties [1], [2].

A typical example of a promising high performance application of GaN-based devices is the AlGaN/GaN heterostructure in high electron mobility transistors (HEMTs). More specifically, the aluminum gallium nitride (AlGaN)/GaN compound system exhibits a large band gap (GaN 3.4 eV, aluminum nitride (AlN) 6.2 eV), a high saturated drift velocity of electrons ($2.2x10^7$ cm/s), a high breakdown electric field ($1–3x10^{10}$ V/cm) and good thermal stability properties [3]. These properties make this system an ideal candidate for electronic and optoelectronic applications. Moreover, the large conduction band discontinuity and strong spontaneous and piezoelectric polarization effect that it presents, induce a 2-dimensional electron gas (2DEG) near the interface (without any intentional doping), making it ideal for HEMT implementation [4].

Due to the fact that native substrates of GaN are still very expensive [5], the growth of GaN and related materials is mostly carried out on various foreign substrates such as sapphire (α-A_2O_3), silicon (Si) and silicon carbide (SiC) [6]. Because of the availability and relatively low cost, GaN-based devices are normally grown on sapphire substrates. However, their lattice parameter and thermal expansion coefficient (TEC) are significantly different from those of GaN.

For power device applications, however, SiC is the most suitable substrate for GaN heteroepitaxy, exhibiting many interesting properties surpassing those of sapphire or silicon: a higher thermal conductivity (3.7 W/(cm·K)) (almost one order of magnitude greater than that of sapphire) and a lower lattice mismatch to GaN (about 3.4%) and AlN (<1%) [7]. However, even this relatively small lattice mismatch combined with the TEC mismatch can result in crystalline defects and bowing of the epitaxial wafers, degrading the device performance. A usual problem that occurs during the growth of GaN directly on (0001) SiC substrates is that GaN is under tensile strain, resulting in a high dislocation density and even the occurrence of cracks in the GaN epilayer.

Therefore, many studies have been conducted to the growth of GaN-based electronic devices on *off-axis* SiC. However, as the SiC substrate size has already reached 6-inch, even a 4° off-cut significantly increases the wafer cost [8]. Therefore, nowadays the research is directed to the growth of AlGaN/GaN heterostructures onto 2 degrees off axis 4H-SiC substrates.

In this work, we report on the structural characterization of AlGaN/GaN heterostructures grown on 4H-SiC (0001) substrates by the metalorganic vapor phase epitaxy (MOVPE) method. Two types of substrates were used: on axis and 2° off cut. The structural characterization was performed by using conventional and high-resolution Transmission Electron Microscopy (TEM and HRTEM) as well as Scanning Transmission Electron Microscopy (STEM), combined with Energy Dispersive X-ray analysis (EDS).

2. Experimental

The epitaxial growth of the multilayer structures on (0001) 4H-SiC substrates was carried out by using an EMCORE Turbodisc™ D75 metalorganic chemical vapor deposition (MOCVD) system operating at low pressures. Trimethylgallium (TMG), trimethylaluminum (TMA), and ammonia (NH3) were used as Ga, Al and N precursors, respectively. Before the growth initiation, the substrates were cleaned using solvents, and then subjected to an in-situ thermal cleaning in flowing H_2 at 1100^{o}C for 10 min.

At first, an AlN nucleation layer was deposited, on which the AlGaN/GaN heterostructures were grown in sequence of a GaN buffer layer and an AlGaN (21% Al) barrier layer. During the growth of AlN and AlGaN, the reactor pressure was maintained at 70 mbar to reduce parasitic reactions and increase the incorporation efficiency of Al into the AlGaN films. All layers were grown with unintentional doping. An extra AlN spacer layer was deposited in between the AlGaN/GaN heterostructure. Finally, a GaN cap layer was deposited on top of the HEMT structure.

Two sets of samples were grown on 4H-SiC substrates, consisting of six different layers: Sample-A on almost “on axis” 4H-SiC (±0.5°) and Sample-B on 2° off axis from the (0001) plane. The layer sequence of the epi-structures is described in Table 1 (from bottom to top).

The structural characterization of the MOVPE-grown specimens was carried out by using a JEOL 2011 electron microscope operated at 200 kV. High Angle Annular Dark-Field-STEM (HAADF-STEM) images and EDS elemental maps were acquired by using an aberration-

corrected 'cubed' FEI Titan 60-300 electron microscope operated at 300 kV, equipped with the ChemiSTEM system [9]. TEM specimens were prepared using traditional methods, including mechanical polishing and argon ion-milling, as for example described in [10].

Table I
Nominal and measured thicknesses of the samples examined.

Layers Numbering	Layers (bottom to top)	Nominal thickness (nm)	Experimental thickness (nm) *A-Sample* ±0.5 deg off	Experimental thickness (nm) *B-Sample* 2 deg off
	Substrate		**4H-SiC**	**4H-SiC**
1	AlN nucleation layer	60-90	14-35	11-38
2	GaN buffer	1720	1830-1850	1580-1600
3	GaN undoped channel	80		
4	AlN spacer	1	1.5-3.5	3-5
5	AlGaN (~20%Al)	20	22-31	19-21
6	GaN cap	2-2.5		

3. Results and discussion

For all samples electron diffraction analysis reveals a strong epitaxial relationship between the epilayers and the 4H-SiC substrate, besides the lattice mismatch at the interface plane. A typical example from an area containing the 4H-SiC substrate as well as the first grown layers of Sample-B is shown in Fig. 1. The following epitaxial relationship is deduced:

$[0001]_{SiC}//[0001]_{GaN}$, $[1\bar{1}00]_{SiC}//[1\bar{1}00]_{GaN}$ and $[11\bar{2}0]_{SiC}//[11\bar{2}0]_{GaN}$

The main reflections of the two phases are indicated by white arrows; the SiC reflections are denoted in italic. The c/a ratio is found to be 1.61 (for GaN), in good agreement with the value 1.63 referred to in the literature. The AlN reflections are very weak due to the small thickness of the layer and moreover they are very close to those of GaN and 4H-SiC. They are only detected far away from the central beam, as shown in the inset of Fig. 1.

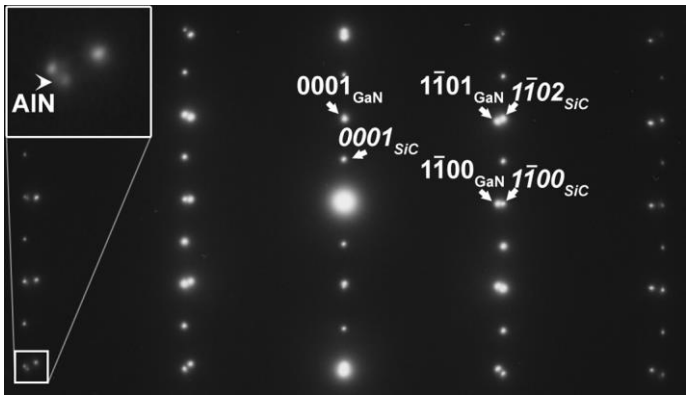

Fig. 1: A typical electron diffraction pattern obtained from a selected area containing part of the 4H-SiC substrate and the first grown layers along [11$\bar{2}$0]. The very good epitaxial growth of GaN layers on the 4H-SiC substrate is clear.

For a structural characterization of the epilayers and interfaces cross-sectional TEM samples were prepared. The conventional bright field images in Fig. 2 (a) and (b) show the multilayer structure of Sample-A and B, respectively; the layer thicknesses (nominal and experimental) of the epi-structures are given in Table 1 (from bottom to top). This table shows that in most of the layers the thickness decreases, as the misorientation angle increases. This trend can be easily explained by a potential growth rate difference (as in the work of Rudzinski et al. [11]) for samples grown under the same conditions (in the same growth run).

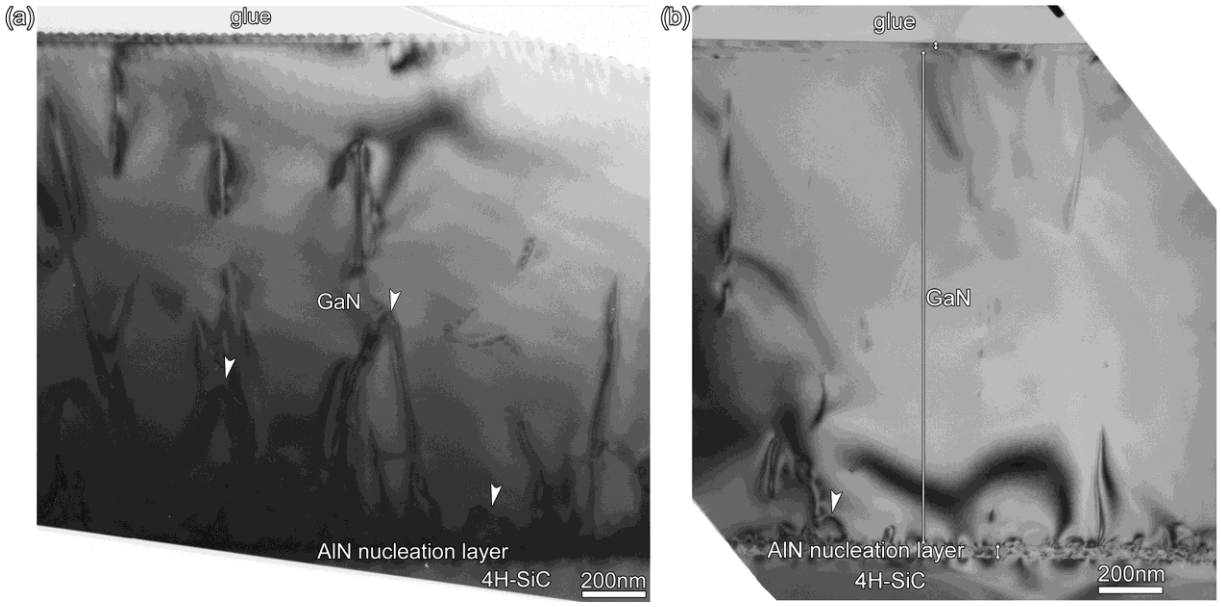

Fig. 2: Low magnification TEM images showing the multilayer structures grown on (0001) 4H-Si substrates for (a) Sample-A and (b) Sample-B.

In both images of Fig. 2 defects -mostly dislocations- are observed. They start from the AlN/GaN interface and expand towards the surface of the structure. The threading dislocation (TD) density in the GaN layer of Sample-A is ~$9 \cdot 10^9 cm^{-2}$, larger than the one measured in the off axis sample case of Sample-B ($\sim 3.5 \cdot 10^9 cm^{-2}$), probably due to strain relaxation [12], [13]. Generally, the strain relaxation mechanisms involved are dependent on the substrate miscut angle. According to J. Pernot et al. [14], in the on axis case, during AlN nucleation layer growth, the coalescence of misoriented islands could have resulted in TD formation, relaxing the strain. On the other hand, during AlN nucleation layer growth in the off axis case, the island formation is limited and thus the isolated threading dislocation density is also limited. In this case, a step flow growth is favored, and other relaxation mechanisms appear (in forms of various types of dislocations and stacking faults formation) [14].

The initially high TD density at the AlN/SiC interface is gradually reduced as the GaN film continues to grow. Closed dislocation loops are observed in both cases (noted by arrows in Fig. 2), being more abundant in the on axis sample. As reported in [15], TDs bend into the basal plane; react with dislocations of the opposite phase and are eliminated by forming closed loops in the AlN nucleation layer and in the lower regions of the GaN epilayer. Therefore, the dislocations do not propagate to the upper part of the GaN epilayer, inducing a higher crystal quality GaN epilayer. Obviously, a high crystalline quality of the epilayers is advantageous for obtaining better AlGaN/GaN heterostructures and thus device performance [7].

In the following paragraphs we will discuss the microstructure of the different layers, starting from bottom to top.

- **Steps in the 4H-SiC/AlN nucleation layer interface**

Fig. 3 presents a typical HRTEM image of the AlN nucleation layer/4H-SiC interface for Sample-B (2° cut-off). The surface of the 4H-SiC substrate consists of (0001) atomically flat and smooth terraces with periodic one atomic layer steps of 2.5 Å (white arrows in Fig. 3). Moreover, the steps are perpendicular to the $[11\bar{2}0]$ direction (or aligned along the $[1\bar{1}00]$ direction) and the distance between the steps is about 6 nm, in agreement to the 2° off-cut. As the

step density is high and the terraces are not too long, incorporation of aluminum (Al) and nitrogen (N) takes place at the step edges during growth, whereas growth on the terraces is limited. Thus, step flow growth is induced initiating from the steps positions, with a direction determined by the step orientation [11].

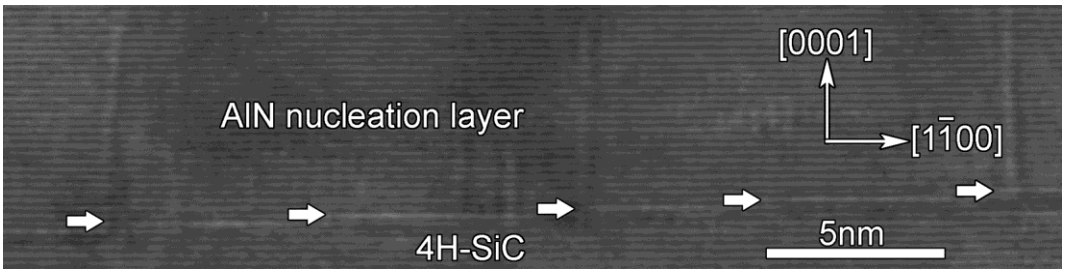

Fig. 3: A HRTEM image indicating the steps in the 4H-SiC/AlN nucleation layer interface (Sample-B).

On the other hand, in the (almost) on axis case, the 4H-SiC/AlN interface is almost free of steps. Therefore, the growth initiation on the "on-axis" substrate surfaces is random and the growth direction is not determined by the step orientation [11].

Furthermore, in 2° off-cut substrates, the growth on the step positions, inherits the stacking order from the substrate. However, the step height is affected by the 4H-SiC substrate with the lattice constants differences being very small in order to be affected by the AlN epilayer. More specifically, the monolayer distance along the c-axis of 4H-SiC is ~2.51Å and for AlN ~2.49Å. Thus, stresses are induced at the step positions. Moreover, due to the unit cell difference, defects are generated in the AlN nucleation layer starting at the step positions, (see the vertical change in contrast in Fig. 3).

In Sample A, with a slight miscut of ±0.5°, a small number of such defects exist, however, the residual off-cut still results in a small number of steps and so leads to a small but important defect density [11]. Moreover, in this case, defects could also be formed due to the orientation mismatch at the grain boundaries between the different AlN grains, formed during growth on the substrate surface. The AlN grain size strongly depends on the AlN layer thickness, so a thickness of 35nm could result in a large number of small not fully coalesced AlN grains, forming defects starting from this epilayer and extending into the GaN layer.

- **V- shaped structures in the AlN nucleation layer**

The AlN nucleation layer thickness does not exceed 40nm, i.e. is too thin to accommodate the stress induced due to TEC mismatch and no cracks are observed in the epilayers. This is compatible with ref. [7], [16], where they reported the growth of a AlN buffer layer of 100nm thickness on SiC substrate showing a 70% relaxation degree and of 150nm thickness nearly fully relaxed.

An AlN buffer layer has been widely used to reduce the tensile strain, important for a smooth GaN layer surface with a low threading dislocations density for samples grown by MOCVD. As reported by Lahreche et al. [17], the growth of GaN directly on SiC substrates results in a rough, islanded GaN layer due to poor surface wetting, deteriorating the GaN film quality. For this reason, Lie et al. [18] have reported the use of an AlN buffer layer, prior to GaN growth, as a good wetting agent on the SiC substrate. Moreover, the use of a AlN layer before GaN growth serves as an intermediate layer with a smaller lattice mismatch with SiC (reducing it from -3.9% to -2.4%).

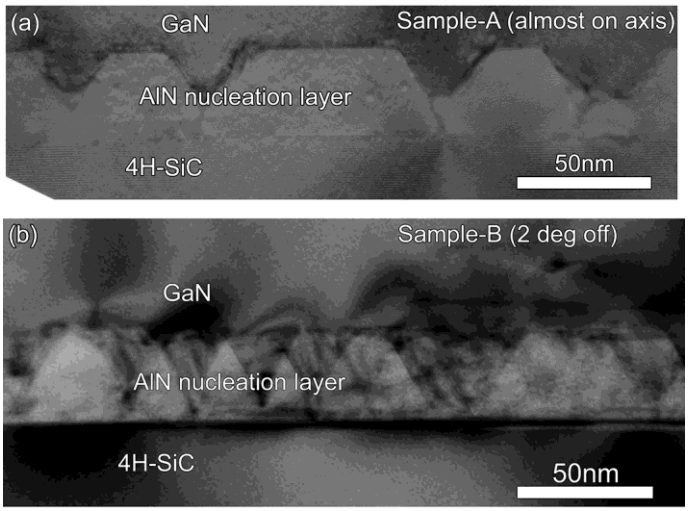

Fig. 4: TEM images of the GaN/AlN/SiC interfaces for a) Sample-A and b) Sample-B. V-shaped defects are grown into the AlN nucleation layer.

As shown in Fig. 4 (a) and (b), the AlN nucleation layer with a thickness of about 35 nm is composed of not completely, but partially, coalesced V-shape formations with random size. The sides of these defects appear to be aligned with specific crystallographic directions. More specifically, they mostly present an angle of about 60°, with $\{1\bar{1}01\}$ sidewalls. V-shaped defect widths between 20 and 45 nm are observed for both samples and their depth is about 20-25 nm. However, they are flat-topped, better defined and of smaller size for the on-axis sample (Fig. 4a).

Probably, the increase of the AlN thickness (from 35 nm for Sample-A to 38 nm for Sample-B) results in a small increase of the V-shape defect size.

According to the interpretation given in [19], the V-shaped formations seem to have grown laterally and vertically with different growth rates, with a higher vertical as compared to the lateral-sidewalls growth rate. More specifically, a reduced Al incorporation (and thus growth rate) on the reversed pyramid walls $\{1\bar{1}01\}$ in comparison with the (0001) planes probably resulted in this defect formation. It has been also reported that threading dislocations can initiate the formation of V-shaped defect [20]–[22]. In our case, the steps existing in the 4H-SiC/AlN interface could easily enhance the V-shape formation, combined with the slow growth rate on $\{1\bar{1}01\}$ facets [23].

- **GaN/AlN nucleation layer area analysis**

In order to precisely determine the distribution of the elements in the region of the V-shaped defects, HAADF-STEM images and STEM-EDS elemental maps were acquired. In HAADF-STEM mode the scattering is Rutherford-like and therefore the intensity of the images is proportional to the atomic number Z^n ($1.6 < n < 2$) [24] and scales with the thickness of the sample. Consequently, higher Z elements will look brighter in the image compared to the lighter ones. Since the Ga atomic number is higher compared to Al, the bright contrast V-shaped defect in Fig 5. corresponds to GaN. Indeed, the STEM-EDS analysis of Fig. 6 confirmed the elemental composition in the V-shaped defect area. More specifically, GaN is found to have started growing into the V-shaped defects formed in the AlN nucleation layer, although Al is not completely absent in this area. This confirms the presence of AlGaN areas in the walls of the V-defect, which is also clearly present in the HAADF-STEM image of Fig. 5 as grey areas (indicating inter-diffusion between the layers). However, pure GaN exists as we move towards the surface of the structure, inside the V-shaped defect. Thus, the V-shaped defects formed into the AlN nucleation layer, are completely overgrown by GaN during the subsequent layer deposition.

The higher contrast layer present at the AlN/SiC interface in the HAADF-STEM image of Fig. 5, indicates the presence of a higher atomic number element, which, based on the EDS analysis results (Fig. 6) is proved to be Ga. This fact is also confirmed by the line scan and the EDS

spectrum results (see supporting information). In the line scan graph, an interdiffusion situation is also indicated, due to the fact that a small Ga quantity is present in the AlN nucleation layer. Moreover, as indicated by the EDS analysis of Fig 6, the V-shaped defect walls are composed of AlGaN, with a decreasing Al content as moving inside the V and towards the structure surface.

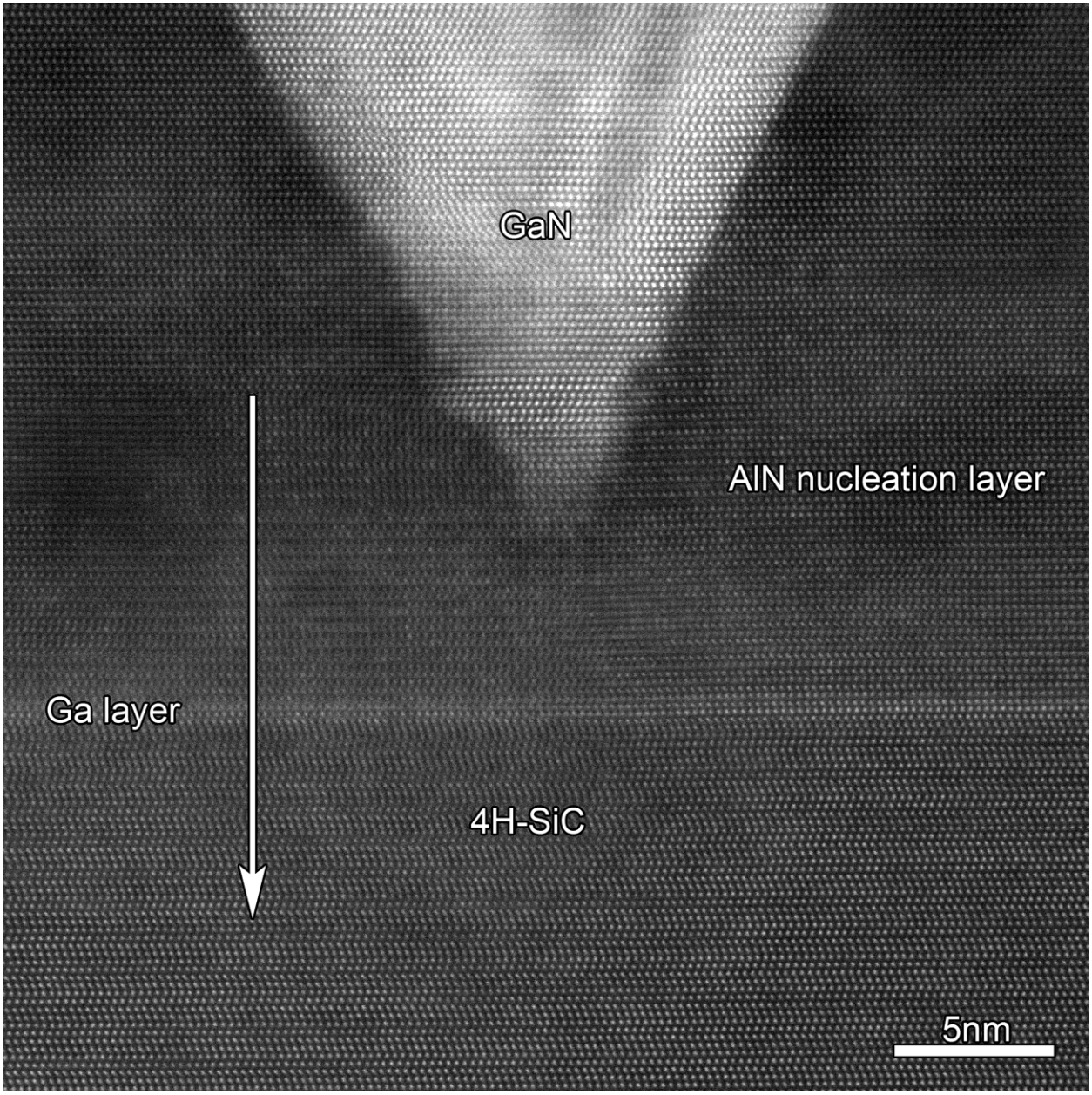

Fig. 5: A HAADF-STEM image showing a characteristic V-shaped formation grown in the AlN nucleation layer. The characteristic alteration in contrast on the substrate surface reveals the presence of a layer consisting of an element with higher atomic number; in this case Ga (see Fig. 6).

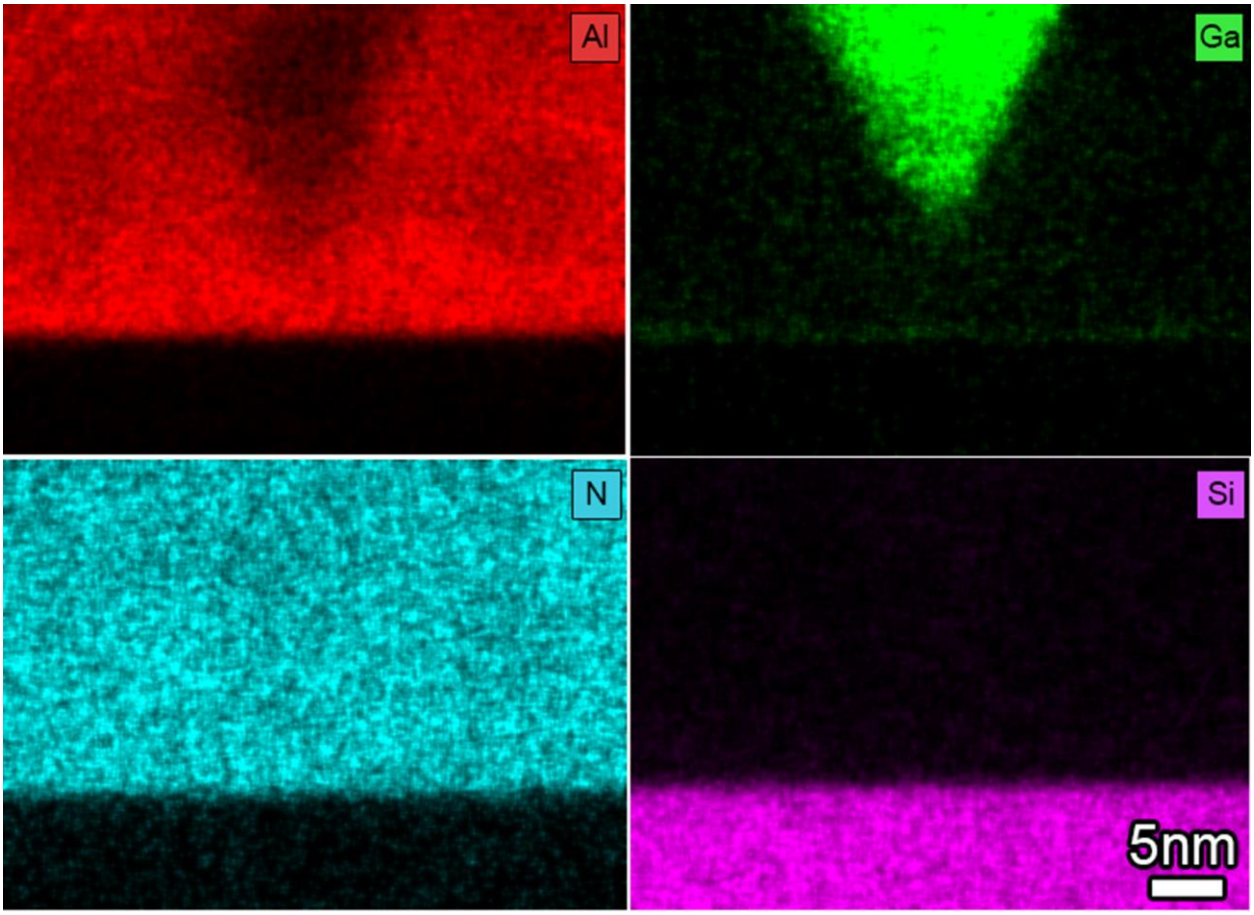

Fig. 6: STEM-EDS analysis revealing the distribution of the elements at the region of the V-shaped defect of Fig. 6. The interdiffusion at the walls is obvious.

In addition, in both cases, an almost smooth surface of the overgrown GaN is observed (Fig. 10). Due to the thick GaN layer (1.6-1.8 μm) grown over AlN, the initially isolated GaN islands coalesced resulting in a smooth surface. Similarly to this study Davis et al. [25] and Nishida et al. [26] observed that a GaN layer grown on AlN buffer layers exhibits similar surface features as the layer on which they are grown and that the preferential nucleation sites of GaN islands are the undulations-pits of the AlN surface.

- **Surface of multilayer structure**

After the thick GaN buffer layer growth, the GaN/AlGaN heterostructure is deposited, with an AlN spacer layer grown in between. By magnifying the upper part of the structure shown in the

TEM image of Fig. 2, the free surface is clearly observed. In the HRTEM images of Fig. 10 (a) and (b), the surfaces of Samples-A and B are shown. In Sample-A (Fig. 10 (a)), where the structure is grown on an almost on axis substrate, the free surface appears with a characteristic undulation forming V-shaped defects, whereas in Sample-B (with 2^{o} off cut) (Fig. 10 (b)) no such an observation is made. However, in this case, stacking faults are formed, as observed in the HRTEM image of Fig. 10 (b) [27]. The elemental composition of the upper layers of Sample-B is shown in Fig. 11; the STEM-EDS map confirms the presence of an Al-enriched layer in between the AlGaN/GaN heterostructure as well as the presence of the GaN cap layer on top of the structure.

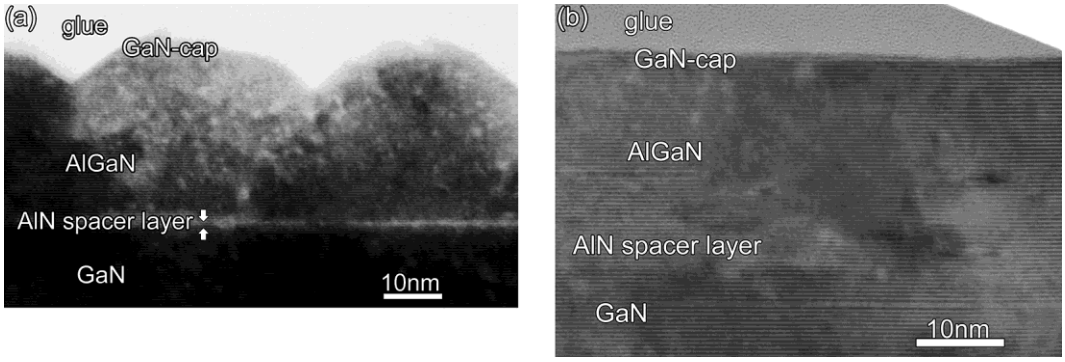

Fig. 7: HRTEM images showing the surface of the multilayer structure for a) Sample-A, showing V-shaped defects and for b) Sample-B, showing an almost sharp surface.

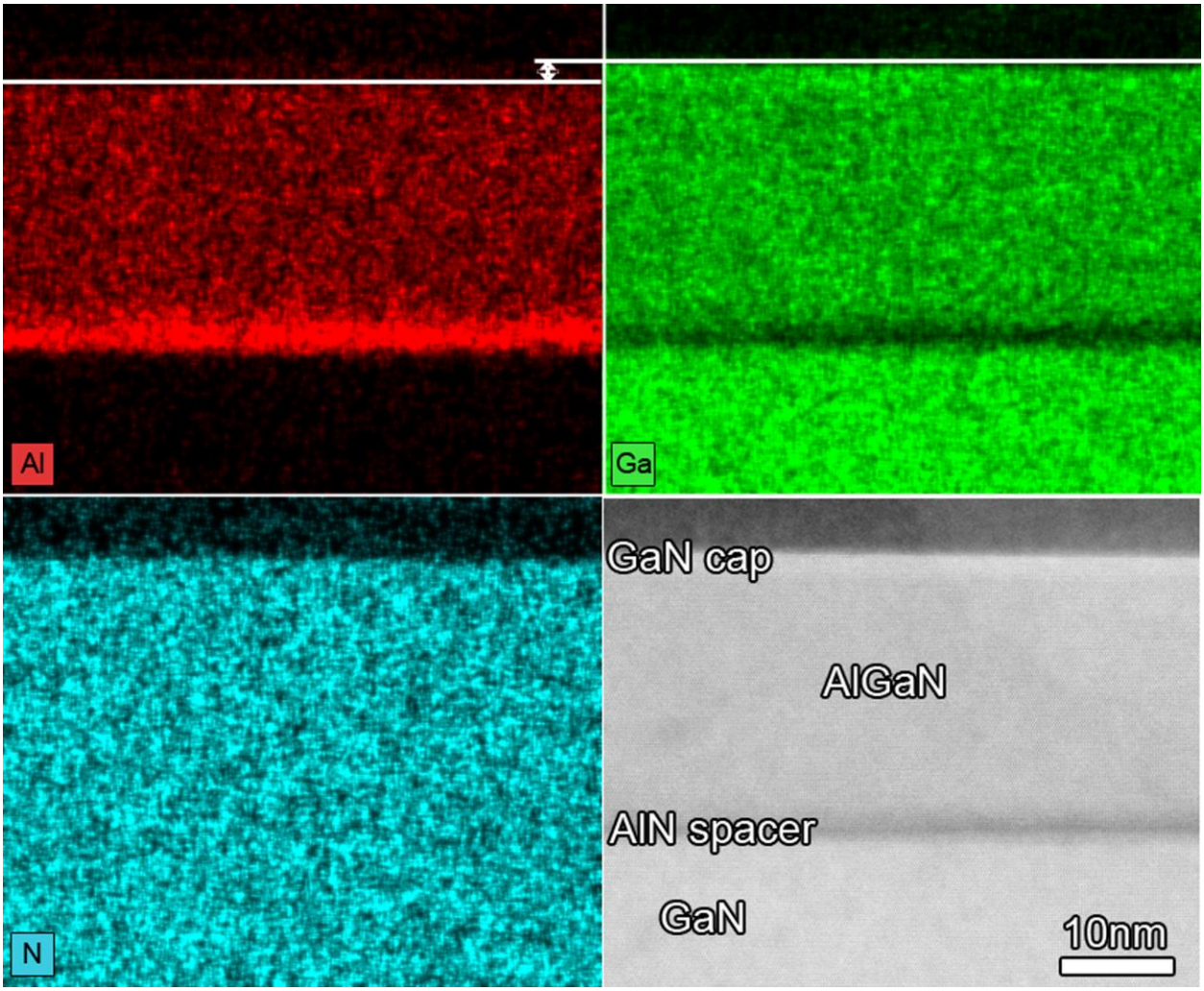

Fig. 8: STEM-EDS analysis showing the elemental composition of the upper layers of the multilayer structure of Sample-B. In the Al and Ga mapping (two upper panels of the figure) the AlN spacer (in between the AlGaN/GaN heterostructure) and the GaN cap layers are clearly revealed.

The low Al concentration of the AlGaN layer (21%, less than 25%), should lead to smooth AlGaN surfaces [27]. However, unlike in the work of Cho et al. [27], for the $Al_{0.21}Ga_{0.79}N$/GaN on axis sample, the surface of the $Al_{0.21}Ga_{0.79}N$ layer shows many periodic V-shaped defects. The size of these defects is small, with an average diameter of 5 nm and an average height of 6 nm. The angle of the sidewalls is around 110^{o}. The presence of the V-shaped defects can be attributed to the fact that the AlGaN layer thickness (together with the GaN cap layer-not clearly visible in our TEM images, which has a nominal thickness of 2-2.5 nm) is 22.3-30.8 nm. As a result, the AlGaN layer thickness exceeds the critical thickness and so V-shaped defects are created for strain relaxation reasons. Actually the critical thickness is exceeded due to the combined action of the AlN spacer with the AlGaN and GaN cap. On the other hand, in Sample-

B, the total AlGaN/GaN cap thickness is no more than 21nm. Therefore no relaxation occurs in the form of V-shaped defect creation. Note that this feature is independent of the substrate used for growth.

As already reported [28], it is important to obviate any AlGaN relaxation, for a maximal electron density achievement in the 2DEG (2 Dimensional Electron Gas) channel, determined by the strain via the Al content of the $Al_xGa_{1-x}N$ layer and by the thickness of this layer. In this way, after a certain critical AlGaN thickness, relaxation and stress reduction will set in, negatively affecting the 2DEG density and also the sheet resistance [29]. Moreover, according to other studies, the origin of these defects could be threading dislocations [20]–[22] or basal stacking faults (BSF) combined with stacking mismatch boundaries (SMB) [30].

We should also note that the upper GaN cap layer, grown for passivation reasons, with a thickness not exceeding 3nm, exhibits similar features and follows the morphology of the underneath AlGaN layer grown onto.

- **The AlN spacer layer**

Similarly to previous works [31], a thin AlN spacer layer (with nominal thickness 1 nm) was inserted after the growth of GaN and prior to the growth of AlGaN barrier layer in order to enhance the heterostructure interface and improve the electrical properties of the structure. The HRTEM image of Fig. 12 reveals the growth of the AlN spacer layer in between the AlGaN/GaN heterojunction. This layer does feature an almost uniform thickness and clear interfaces with the AlGaN and GaN layers (the same trend is followed in both samples) [32], although the measured AlN thickness in some of the cases reached ~4.5 nm exceeding the nominal one (1nm). A future electrical characterization study could clearly determine the electronic properties of the 2DEG formed in the AlGaN/GaN heterostructure and the effect of the AlN spacer layer presence. As already reported by Smorchkova et al. [31], the growth of a thin (~1nm) AlN layer between $Al_xGa_{1-X}N$ (x~0.2-0.45) and GaN with thick AlGaN barrier layers (~20-25nm) does not affect the 2DEG sheet density but results in a low-temperature electron mobility increase.

Conclusions

We studied the structural characteristics of AlGaN/GaN multilayer structures epitaxially grown on on-axis and 2° off 4H-SiC substrates. The very good epitaxial growth of the layers, one on top

of the other, was revealed by electron diffraction measurements. In both cases, the GaN epilayer is free of cracks but the "on axis" substrate shows a higher density of TD as compared to the misoriented one. However, in both cases the dislocation density decreases drastically towards the structure surface (forming dislocation loops in the lower regions of GaN). Characteristic V-shaped formations are grown into the AlN nucleation layer (with $\{1\bar{1}01\}$ sidewalls), completely overgrown by GaN in both samples; they are smaller and better defined in the on axis sample. Moreover, the V-shape density is larger in the off axis case, probably due to the higher step density. A defect development is observed at the step positions of the 4H-SiC/AlN interface in the case of 2° off substrates.- Defects are also formed due to the orientation mismatch between the different AlN grains (island growth mechanism). The presence of the Ga layer in the 4H-SiC/AlN interface, could be interpreted by a sort of memory effect. Moreover the only other reason explaining this Ga layer presence would be a kind of an inter-diffusion situation via the AlN nucleation layer that takes place under the specific growth conditions. The AlGaN layer of the AlGaN/GaN heterojunction in the on axis sample, exceeding the critical thickness, presents a characteristic undulation in the form of V-shaped formations, due to strain relaxation. The off-cut sample gives the best morphology (atomically flat) of the AlGaN layer, despite the step bunching. Thus, the use of 2° off 4H-SiC substrates for GaN based-devices epitaxy is perfectly possible.

Acknowledgements

Funding: This work was supported by the IKY Fellowships of Excellence for Postgraduate Studies in Greece-SIEMENS Program; the Greek General Secretariat for Research and Technology, contract SAE 013/8-2009SE 01380012; and the JU ENIAC Project LAST POWER Large Area silicon carbide Substrates and heteroepitaxial GaN for POWER device applications [grant number 120218]. Also part of the research leading to these results has received funding from the European Union Seventh Framework Program under Grant Agreement 312483 - ESTEEM2 (Integrated Infrastructure Initiative–I3). T.A. acknowledges financial support from the Research Foundation Flanders (FWO, Belgium) through a post-doctoral grant.

Supporting Information

The presence of Ga is also confirmed by the line scan results (Fig. SI1). The scanning direction is indicated by a white arrow in the HAADF-STEM image of Fig. 5. It is also revealed that some Ga is present in the AlN nucleation layer (small enough, but detectable), indicating an interdifussion situation. The EDS spectrum of Fig. SI2 clearly states the Ga presence at the AlN/SiC interface.

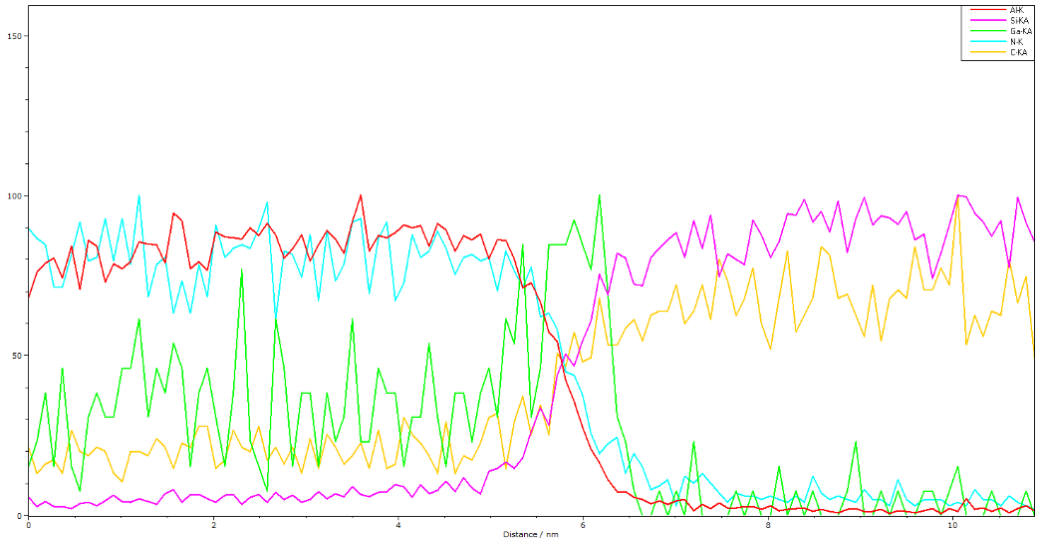

Fig. SI1: Line scan revealing the distribution of the elements. The white arrow at the HAADF-STEM image of Fig. 5 indicates the direction of the scan.

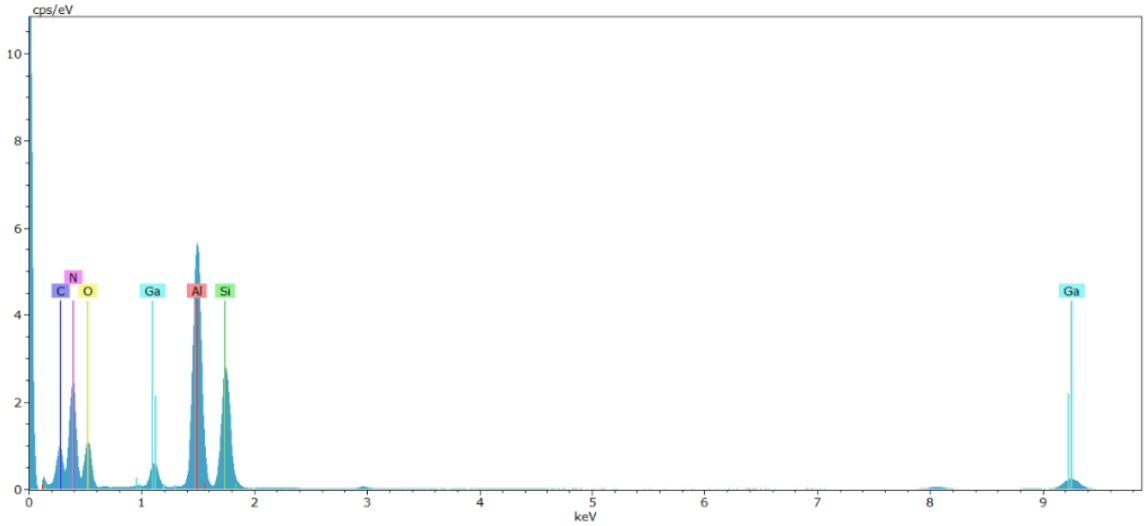

Fig. SI2: EDS spectrum acquired from the region shown in Fig. 5, revealing the elements that are present.

References

[1] S. J. Pearton and F. Ren, "GaN electronics," *Adv. Mater.*, vol. 12, no. 21, pp. 1571–1580, 2000.

[2] M. A. Khan, A. Bhattarai, J. N. Kuznia, and D. T. Olson, "High electron mobility transistor based on a GaN- Al x Ga1−x N heterojunction," *Appl. Phys. Lett.*, vol. 63, no. 9, pp. 1214–1215, 1993.

[3] N.-Q. Zhang, S. Keller, G. Parish, S. Heikman, S. P. DenBaars, and U. K. Mishra, "High breakdown GaN HEMT with overlapping gate structure," *IEEE Electron Device Lett.*, vol. 21, no. 9, pp. 421–423, Sep. 2000.

[4] W. Luo *et al.*, "Growth and fabrication of AlGaN/GaN HEMT based on Si (111) substrates by MOCVD," *Microelectronics J.*, vol. 39, no. 9, pp. 1108–1111, 2008.

[5] T. Paskova, D. A. Hanser, and K. R. Evans, "GaN substrates for III-nitride devices," *Proc. IEEE*, vol. 98, no. 7, pp. 1324–1338, 2010.

[6] P. Rudolph, *Handbook of Crystal Growth: Bulk Crystal Growth*, vol. II. 2015.

[7] D. Guojian *et al.*, "Characteristics of GaN grown on 6H-SiC with different AlN buffers," *J. Semicond.*, vol. 31, no. 3, p. 33003, 2010.

[8] M. Leszczynski *et al.*, "Potentialities of AIGaN/GaN heterostructures grown on 2°-off 4H-SiC substrates," *Mater. Sci. Forum*, vol. 806, 2015.

[9] P. Schlossmacher, D. O. Klenov, B. Freitag, and H. S. von Harrach, "Enhanced Detection Sensitivity with a New Windowless XEDS System for AEM Based on Silicon Drift Detector Technology," *Micros. Today*, vol. 18, no. 4, pp. 14–20, 2010.

[10] L. M. Sorokin, A. V. Myasoedov, A. E. Kalmykov, D. A. Kirilenko, V. N. Bessolov, and S. A. Kukushkin, "TEM investigation of semipolar GaN layers grown on Si (001) off cut substrates," *Semicond. Sci. Technol.*, vol. 30, no. 11, p. 114002, 2015.

[11] M. Rudziński *et al.*, "Defect formation in GaN grown on vicinal 4H-SiC (0001) substrates," *Phys. Status Solidi Appl. Mater. Sci.*, vol. 204, no. 12, pp. 4230–4240, 2007.

[12] M. Rudziński *et al.*, "Influence of the misorientation of 4H-SiC substrates on the morphology and crack formation in hetero epitaxial MOCVD grown GaN epilayers," *Phys. Status Solidi C Conf.*, vol. 2, no. 7, pp. 2141–2144, 2005.

[13] K. Matsushita *et al.*, "Influence of SiC Substrate Misorientation on AlGaN/GaN HEMTs Performance," in *CS Mantech Conference*, 2009, pp. 1–4.

[14] J. Pernot, E. Bustarret, M. Rudziński, P. R. Hageman, and P. K. Larsen, "Strain relaxation in GaN grown on vicinal 4H-SiC(0001) substrates," *J. Appl. Phys.*, vol. 101, no. 3, p. 33536, 2007.

[15] M. M. Muhammed *et al.*, "High-quality III-nitride films on conductive, transparent ($\bar{2}01$)-oriented β-Ga2O3 using a GaN buffer layer," *Sci. Rep.*, vol. 6, no. April, p. 29747, 2016.

[16] B. Moran, F. Wu, A. Romanov, U. Mishra, S. Denbaars, and J. Speck, "Structural and morphological evolution of GaN grown by metalorganic chemical vapor deposition on SiC substrates using an AlN initial layer," *J. Cryst. Growth*, vol. 273, no. 1–2, pp. 38–47, 2004.

[17] H. Lahrèche *et al.*, "Comparative study of GaN layers grown on insulating AlN and conductive AlGaN buffer layers," *Semicond. Sci. Technol.*, vol. 14, no. 11, pp. L33–L36, 1999.

[18] L. Liu and J. H. Edgar, "Substrates for gallium nitride epitaxy," *Mater. Sci. Eng. R Reports*, vol. 37, no. 3, pp. 61–127, 2002.

[19] X. H. Wu *et al.*, "Structural origin of V-defects and correlation with localized excitonic centers in InGaN/GaN multiple quantum wells," *Appl. Phys. Lett.*, vol. 72, no. 6, pp. 692–694, 1998.

[20] N. Sharma, P. Thomas, D. Tricker, and C. Humphreys, "Chemical mapping and formation of V-defects in InGaN multiple quantum wells," *Appl. Phys. Lett.*, vol. 77, no. 9, p. 1274, 2000.

[21] T. Kehagias *et al.*, "Indium migration paths in V-defects of InAlN grown by metal-organic vapor phase epitaxy," *Appl. Phys. Lett.*, vol. 95, no. 7, 2009.

[22] C. Bazioti *et al.*, "Defects, strain relaxation, and compositional grading in high indium content InGaN epilayers grown by molecular beam epitaxy," *J. Appl. Phys.*, vol. 118, no. 15, 2015.

[23] Z. Liliental-Weber, Y. Chen, S. Ruvimov, and J. Washburn, "Formation Mechanism of Nanotubes in GaN," *Phys. Rev. Lett.*, vol. 79, no. 15, pp. 2835–2838, 1997.

[24] S. J. Pennycook, "Z-contrast stem for materials science," *Ultramicroscopy*, vol. 30, no. 1–2, pp. 58–69, 1989.

[25] R. F. Davis, S. Einfeldt, E. A. Preble, A. M. Roskowski, Z. J. Reitmeier, and P. Q. Miraglia, "Gallium nitride and related materials: Challenges in materials processing," *Acta Mater.*, vol. 51, no. 19, pp. 5961–5979, 2003.

[26] T. Nishida and N. Kobayashi, "Nucleation control in MOVPE of group III-nitrides on SiC substrate," *J. Cryst. Growth*, vol. 221, no. 1–4, pp. 297–300, 2000.

[27] H. K. Cho and J. Y. Lee, “Formation of V-Shaped Pits in Nitride Films Grown by Metalorganic Chemical Vapor Deposition,” vol. 42, no. February, pp. 547–550, 2003.

[28] O. Ambacher *et al.*, “Two-dimensional electron gases induced by spontaneous and piezoelectric polarization charges in N- and Ga-face AlGaN/GaN heterostructures,” *J. Appl. Phys.*, vol. 85, no. 6, p. 3222, 1999.

[29] K. Cheng *et al.*, “Formation of V-grooves on the (Al,Ga)N surface as means of tensile stress relaxation,” *J. Cryst. Growth*, vol. 353, no. 1, pp. 88–94, 2012.

[30] J. Smalc-Koziorowska, E. Grzanka, R. Czernecki, D. Schiavon, and M. Leszczyński, “Elimination of trench defects and V-pits from InGaN/GaN structures,” *Appl. Phys. Lett.*, vol. 106, no. 10, 2015.

[31] I. P. Smorchkova *et al.*, “AlN/GaN and (Al,Ga)N/AlN/GaN two-dimensional electron gas structures grown by plasma-assisted molecular-beam epitaxy,” *J. Appl. Phys.*, vol. 90, no. 10, pp. 5196–5201, 2001.

[32] Y. Y. Wong *et al.*, “Growth and fabrication of AlGaN/GaN HEMT on SiC substrate,” *2012 10th IEEE Int. Conf. Semicond. Electron. ICSE 2012 - Proc.*, pp. 729–732, 2012.